Thermal conductivity of germanium crystals with different isotopic compositions

M. Asen-Palmer, K. Bartkowski, E. Gmelin, and M. Cardona
Max-Planck-Institut für Festkörperforschung, D-70569 Stuttgart, Germany

A. P. Zhernov, A. V. Inyushkin, A. Taldenkov, and V. I. Ozhogin
Russian Research Center, Kurchatov Institute, 123182 Moscow, Russia

K. M. Itoh* and E. E. Haller
University of California at Berkeley and Lawrence Berkeley Laboratory, Berkeley, California 94720
(Received 28 April 1997)

We have measured the thermal conductivity of seven germanium crystals with different isotopic compositions in the temperature range between 2 K and 300 K. These samples, including one made of highly enriched ^{70}Ge(99.99%), show intrinsic behavior at room temperature with the exception of a p-type sample with $|N_d\text{-}N_a| \cong 2\times10^{16}$ cm^{-3}. The ''undoped'' samples exhibit a T^3 dependence at low temperatures, basically determined by boundary scattering. The maximum value of κ (which falls in the range between 13 K and 23 K) is found to be a monotonically decreasing function of the isotopic mass variance parameter g. The maximum κ_m measured for the most highly enriched ^{70}Ge(99.99%) sample is 10.5 kW/mK, one order of magnitude higher than for natural germanium. The experimental data have been fitted with the full Callaway theory, modified by treating transverse and longitudinal modes separately, using three free adjustable parameters for each set of modes to represent anharmonic effects plus the calculated contributions from isotopic and boundary scattering. For the isotopically purest ^{70}Ge(99.99%) sample, dislocation scattering, or a similar mechanism, must be added in order to fit the data. We have also checked the effect of various surface treatments on the thermal conductivity in the low temperature region. The highest values of κ are found after polish etching with a SYTON suspension. [S0163-1829(97)00539-0]

I. INTRODUCTION

The thermal conductivity of diamondlike semiconductors and insulators, especially of Ge, has been the object of many experimental and theoretical studies.[1–11] Early experiments indicated the existence of a maximum κ_m near $T \approx 0.05\theta$ (θ: Debye temperature) which was attributed to the increase of the thermal conductivity with T in the low temperature region (governed by T-independent boundary scattering and the T^3 dependence of the specific heat), followed by the decrease at higher temperatures due to phonon decay resulting from anharmonic Umklapp processes.[12] Near the maximum, the thermal conductivity κ_m is particularly sensitive to sample imperfections and impurities. In the usual model of the thermal conductivity of insulating materials, in which the heat is carried exclusively by phonons, a Boltzmann equation with a relaxation time approximation is used. In this case the scattering cross sections can be calculated by perturbation techniques.[6,13] In such a treatment, the temperature and frequency dependences of anharmonic three-phonon processes are strongly affected by details of the phonon branch and anharmonicity constants: The expressions derived for the relaxation times are only valid for specific phonons in a limited temperature range.[14,15] Callaway,[16–18] and later Holland,[19] presented the most widely used formulation for $\kappa(T)$ that should enable fitting of the data for a large number of materials with a few adjustable parameters. For undoped and isotopically pure Ge and Si four scattering mechanisms were postulated: Scattering by the sample boundaries, crystal-defects (e.g., impurities), normal three-phonon processes, and Umklapp processes. (For very pure samples scattering by dislocations must also be considered.)

Since the early work of Pomeranchuk,[20] demonstrating the role of isotopes as phonon scatters with a resulting influence on the thermal conductivity, and the work performed by Geballe and Hull[21] it has been known that the maximum thermal conductivity κ_m is strongly affected by the isotopic composition. This fact has received considerable attention in recent years for the case of diamond: An $\approx$1% reduction of the ^{13}C content in natural diamond enhances κ_m (which occurs near liquid nitrogen temperature) by 50%, a useful result if diamond is employed as a substrate for heat dissipation purposes.[22–24] Geballe and Hull observed an increase in the κ_m of an enriched ^{74}Ge sample (with 95.8% of ^{74}Ge) by a factor of 3 with respect to natural germanium.[21]

Many physical properties of a solid are affected by its isotopic composition.[25–28] The recent availability of macroscopic quantities of isotopically pure Ge has enabled the growth of high purity single crystals with tailor-made isotopic compositions.[26,29] This has triggered intensive studies of the optical and vibrational properties (Raman and neutron-scattering, infrared transmission, etc.) of isotopically disordered Ge.[27,30–34] Isotopic substitution does not only modify the average isotopic mass but creates ''perfect'' point defects, producing mass disorder that should drastically influence the phonon lifetime. Natural Ge is ideal for studying such disorder-induced scattering processes because it is composed of *five* isotopes with sizable abundances. Mass defect scattering in an elemental crystal belongs to the rare cases in which phonon scattering can be calculated analytically with-

out stringent assumptions. Klemens[35] derived for such scattering a mean free path $L_I \sim g T^4$, where g denotes the isotopic mass variance:

$$g = \frac{\sum c_i M_i^2 - \left(\sum c_i M_i \right)^2}{\left(\sum c_i M_i \right)^2}. \quad (1)$$

In Eq. (1), c_i and M_i represent the concentration and the mass of the constituent isotopes, respectively.

In the past four decades, however, only few investigations have been reported on the effect of isotopic composition on thermal conductivity. Measurements for LiF,[36] Ge,[21,37,38] and diamond[22,23,39,40] were performed in the temperature range between 4 K and room temperature or higher. Studies of solid ^{4}He,[41,42] LiF,[36,43,44] Ne,[45,46] and B_4C,[47] cover only a rather limited temperature range. Effects similar to those caused by isotopic disorder are produced by very heavy isolated impurities in quantum crystals, e.g., Ar, Ne in parahydrogen.[48,49]

At low temperatures $[T < (\theta/50)]$ the thermal conductivity is proportional to T^3, which corresponds to scattering of phonons at the sample surface (boundary scattering).[50] In this range, further interesting effects that lead to a deviation from the T^3 behavior have been predicted and observed. They involve the dependence of κ on sample dimensions when the length is finite,[51–56] and on sample orientation because of phonon focusing (a result of the elastic anisotropy).[57–59] Also, partly specular reflection[43,52–56,59–63] as obtained for high quality surfaces, and dislocation effects,[2,13,35,53,60,64] can influence the T^3 law.

In this paper we present a systematic investigation of the thermal conductivity for seven samples of germanium, in the temperature range between 2 K and 300 K where the isotopic composition covers the range from highly enriched ^{70}Ge(99.99%) to $^{70/76}$Ge, the composition which exhibits the largest isotopic mass variance g. We show that for the ^{70}Ge(99.99%) sample ($g \approx 1.0 \times 10^{-7}$) κ_m reaches values as high as 10.5 kW/mK, whereas the most disordered composition ($g \approx 1.5 \times 10^{-3}$) displays a 14 times lower thermal conductivity (0.75 kW/mK). We analyze our data in the framework of various models: Callaway's theory,[16] Holland's theory,[19] and a modified Callaway/Holland theory where we distinguish between scattering mechanisms for transverse and longitudinal phonons. The thermal conductivity results for the different samples (we also included the experimental data for ^{74}Ge measured by Geballe and Hull) are then described reasonably well as a function of g using *a single set of six fitting parameters*: Two for normal three-phonon processes (one for longitudinal, another for transverse phonons) and four for transverse and longitudinal Umklapp processes. Two additional parameters which determine boundary and isotopic scattering are not adjusted but fixed by sample size and isotopic composition, respectively.

The theoretical picture shows that normal phonon scattering, rather than Umklapp processes, plays the critical role for the determination of the phonon mean free path for most samples in our temperature range. The isotopic effect, even observed near room temperature, is consistent with the theory.[16,19] For the highly enriched ^{70}Ge(99.99%) sample, an additional process, such as scattering by dislocations, must influence the maximum of the thermal conductivity. We also consider the effects of sample length, specularity, and phonon focusing, and study the influence of different surface conditions (polishing and etching) on the thermal conductivity in the lowest temperature range.

In Sec. II the experimental techniques and the samples used are discussed. Section III presents the experimental results for samples with various isotopic compositions and different surface treatments. These results are analyzed in Sec. IV after outlining the theoretical state of the art. We also discuss the modifications we had to introduce in the theories of Callaway and Holland in order to improve the fits to the experimental data. Finally, the influence of various surface treatments is analyzed. In Sec. V, a discussion of the results is given and in Sec. VI the conclusions are summarized.

II. EXPERIMENTAL DETAILS

The preparation of the Ge samples has been described elsewhere.[26,32] The measured samples and their characteristic parameters are listed in Table I. With regards to doping, sample ^{70}Ge(99.99%) is one of the most perfect Ge crystal ever made, the concentration of electrically active impurities being lower than 10^{11} cm^{-3} (after 33 times zone melting). The $^{70/76}$Ge sample has been grown for the purpose of maximizing isotopic disorder. None of the samples was intentionally doped; they had a carrier concentration of less than 10^{14} cm^{-3} at room temperature, with the exception of ^{70}Ge(95.6%) which had 2×10^{16} holes/cm^3. For details about the surface treatment see Table I (standard was grinding with 20 μm grit diamond powder unless otherwise specified).

The thermal conductivity measurements were made at the Max-Planck-Institute in Stuttgart (the experimental setup is briefly described here) and at the Kurchatov Institute in Moscow, both using conventional equipment.[65,66] A steady-state heat flow Φ is created along the rod-shaped sample with a cross-sectional area A. For this purpose, an electrical heater (a strain gauge, 300 Ω) is attached to one of the sample ends while the other end is in good thermal contact (screwable clamp device with an interlayer of In foil) with a heat sink at variable temperatures. A thermocouple (Au-0.07%Fe) detects the temperature gradient along the sample (in Moscow two calibrated carbon resistors were used instead). The thermal conductivity $\kappa(T)$ at an average temperature $\frac{1}{2}(T_1 + T_2)$ is then calculated from the relation: $\Phi = \kappa(T) A (\Delta T / \Delta x)$, where $\Delta T = T_1 - T_2$ is the temperature difference measured between the two thermometers a distance Δx apart (see Table I) in the presence of the heat flux Φ. The temperature difference between the heater and the heat sink is measured by a second thermocouple (also Au-0.07%Fe) that enables us to evaluate the heat resistance between the sample and the heat sink, to determine the average temperature of the sample (according to sample geometry and temperature of the heat sink), and to control the thermal stability of the system. In all cases, the thermometers were kept at least two sample widths away from the ends of the sample in order not to introduce any significant anomalies in the temperature distribution over Δx. The sample is surrounded closely by a temperature controlled heat-shield kept at the temperature of the heat sink.

TABLE I. Parameters of the Ge samples, with various isotopic compositions, for which $\kappa(T)$ has been measured. The abbreviations O,I denote the principal direction closed to the long axis of the sample and its deviation from this direction. Δx is the distance between the two arms of the differential thermocouple. The variance g is defined in Eq. (1).

	Isotopic Mass Composition [%]							Geometry				Experimental data Thermal conductivity				
	70	72	73	74	76	g (10^{-5})	O/I	a (mm)	b (mm)	l (mm)	Δx (mm)	κ(1.5 K) (W/m K)	κ(3 K) (W/m K)	κ_m (W/m K)	L_E (mm)	Surface treatment
^{70}Ge (99.99%)	99.99	0	0.01	0	0	0.01	100/6°	2.20	2.50	44.5	27.1	32	260	10572	3.6	20 μm diamond (S)
								2.20	2.50	44.5						20 μm diamond (M)
								2.13	2.40	44.5	26.3	68	541	10572	7.5	SYTON (S)
								2.13	2.40	44.5						SYTON (M)
^{74}Ge	0.7	1.1	1.6	95.8	0.8	3.6	100/0°	1.57	1.57	12.0		22	170	3780	2.4	Geballe and Hull (Ref. 21)
^{70}Ge (95.6%)	95.6	3.8	0	0.6	0	4.0	110/27°	5.47	$h=1.6$		6.30	7	57	2315	0.80	$p=2\times10^{16}$ cm^{-3}, 20 μm
								5.15	$h=1.5$	14.0	5.48	11	85	3478	1.2	CP4 (S)
								1.25	1.49	14.0	1.86	7	50	2172	0.70	cut and CP4 (S)
^{70}Ge (96.3%)	96.3	2.1	0.1	1.2	0.3	7.57		2.50	2.50	28.0		36	271	3668	4.0	(M)
^{76}Ge	0	0.1	0.2	13.7	86.0	8.7	100/2°	1.27	2.54	35.0	11.1	29	217	2900	3.2	(S)
^{nat}Ge1	20.5	27.4	7.8	36.5	7.8	58.7	100/0°	2.46	2.50	29.4	6.15	33	211	1368	3.8	20 μm diamond (S)
								2.46	2.50	29.4						20 μm diamond (M)
								2.41	2.44	29.2	5.88	35	220	1368	4.0	3 μm diamond (S)
								2.35	2.40	29.0	5.64	92	495	1650	11	SYTON (S)
								2.30	2.33	29.0	5.36	60	348	1454	7.0	CP4 (S)
^{nat}Ge2	20.5	27.4	7.8	36.5	7.8	58.7	100/0°	1.30	1.30	15.0	8.0	26	173	1286	3.0	SYTON (S)
$^{70/76}$Ge	43	2	0	7	48	153	110/11°	2.02	2.00	23.0	15.6	21	122	741	2.4	CP4 (S)
^{nat}Ge						58.7	100	2.00	2.00	40		28	182		3.2	sandblast (Ref. 52)
							100	1.46	1.45	40		20	137		2.3	sandblast (Ref. 52)
							111	1.46	1.47	40		13	94		1.5	sandblast (Ref. 52)
^{nat}GeI						58.7	100	1.26	1.26	40		19	132		2.2	sandblast (Ref. 52)
^{nat}GeII							100	1.32	1.32	40		43	265		5.0	1 μm diamond (Ref. 52)
^{nat}GeIII							100	1.17	1.17	40		84	461		10	LUSTROX (Ref. 52)
^{nat}Ge						58.7	100	2.53	2.68	50		40	248	1360	4.6	Ref. 6
							100	2.19	2.10	50		30	192	1275	3.4	Ref. 6
^{nat}Ge						58.7		3.95	3.95	24		42	256		4.8	Ref. 7

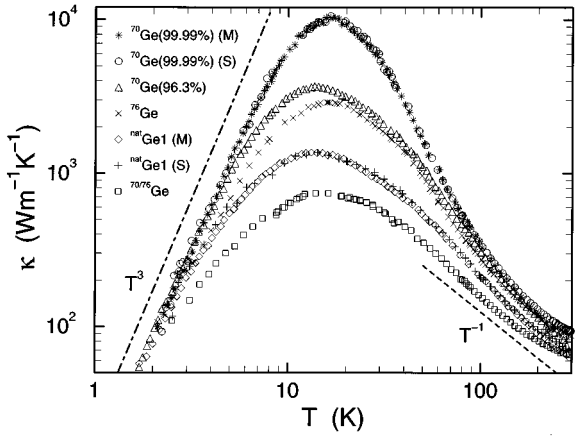

FIG. 1. Thermal conductivity vs temperature of five Ge samples with different isotopic compositions: ^{70}Ge(99.99%), ^{70}Ge(96.3%), ^{76}Ge(86%), ^{nat}Ge1, and $^{70/76}$Ge. Two of the samples ^{70}Ge(99.99%) and ^{nat}Ge1 have been measured with two different experimental setups, in Stuttgart (S) and in Moscow (M). The dot-dashed line represents simply a T^3 law, expected for pure boundary scattering, while the dashed line shows a $1/T$ dependence expected for phonon scattering at high temperatures.

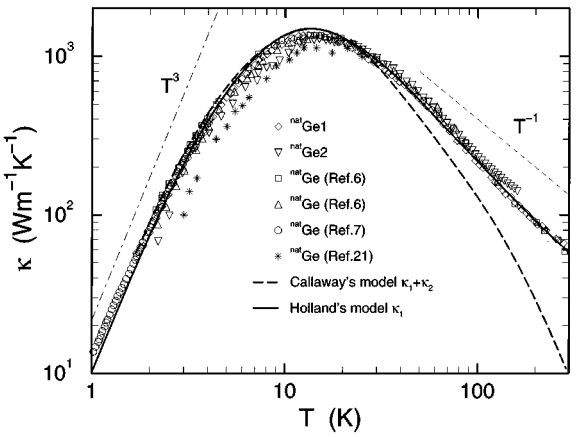

FIG. 2. Thermal conductivity of various [100] oriented natural Ge bars. The dashed line represents the thermal conductivity calculated with the full Callaway model ($\kappa_1+\kappa_2$), where the parameters $B_1=B_2=2.6\times10^{-23}$ s/K^3 are used. The continuous line represents the heat conductivity calculated with the model of Holland (only κ_1), using one single set of parameters for all samples: $B_T=1.5\times10^{-11}$ 1/K^4, $B_{TU}=4.5\times10^{-18}$ s, $B_L=9.0\times10^{-24}$ s/K^3, and $L_E=3.8$ mm, $g=58.7\times10^{-5}$ for ^{nat}Ge1 (see also Tables II and III).

We imposed a temperature gradient along that shield which matches exactly the one in the sample.

The following procedure is employed: ΔT_0 is measured in thermal equilibrium for $\Phi=0$, then the heater is switched on and ΔT is measured for nonzero heat flow. The temperature differences ΔT are held below $0.005T$ for $T>10$ K and 0.01 T for $T<10$ K. Serious errors can occur due to radiative heat loss by heat radiation in the high temperature range ($T>80$ K). To avoid such systematic errors, in addition to using a carefully temperature-controlled heat shield we measured κ at selected temperatures for various heater powers applied to the sample and verified that the law $\Delta T\propto\Phi$ is obeyed. The measurements have an overall absolute accuracy of 5% (the relative error is smaller): Errors due to geometrical factors amount to $\pm3\%$ (dominant error), while ΔT is known to $\pm2\%$.

III. EXPERIMENTAL RESULTS

The thermal conductivities versus temperature measured for various isotopic compositions (see Table I) are displayed as log-log plots in Fig. 1. The data for the isotopically purest sample ^{70}Ge(99.99%) are shown together with results for the less pure ^{70}Ge(96.3%), sample ^{76}Ge(86%), natural Ge, and the most isotopically disordered sample containing 43% of ^{70}Ge and 48% of ^{76}Ge. Both samples, ^{70}Ge(99.99%) and ^{nat}Ge1, were measured with the two different experimental setups, in Stuttgart and in Moscow (results labeled S and M). The S and M data show a striking agreement (to within $\approx1.5\%$) in most of the temperature range. [Between 200 K and 300 K, however, our values of the thermal conductivity lie higher ($\leqslant10\%$) than those obtained in Moscow; because of the nearly perfect agreement between the Moscow data and those in Ref. 5 we believe that our data in this region are less reliable than those taken in Moscow.] The maximum of $\kappa(T)$ amounts to 10.5 kW/mK near 16.5 K for ^{70}Ge(99.99%), which is the highest value of κ measured for Ge, higher than the thermal conductivity maximum of sapphire (6 kW/mK near 35 K) and comparable to that of silver (11 kW/mK near 8 K). Comparable or higher conductivities have been reported for isotopically enriched diamond,[22,23] sapphire,[67] LiF,[36,43] and also for NaF.[68] The isotopically most disordered sample shows, as expected, the lowest thermal conductivity measured for undoped germanium (0.75 kW/mK near 14.5 K). In this sample the isotopic scattering is dominant, in contrast to the pure ^{70}Ge(99.99%) where it becomes negligible. Results for the ^{70}Ge(95.6%) sample, which has a different geometrical size and a much higher carrier concentration than the others (see Table I) is shown later in Fig. 7. Figure 2 displays some of the thermal conductivities of natural Ge so far reported in the literature,[6,7,21] together with our data. With the exception of sample ^{70}Ge(95.6%), all samples have a similar geometry (within 10% equal cross-sectional dimensions and identically prepared surfaces). They were cut with a diamond saw and the surfaces lapped with a 20 μm diamond powder slurry.

The overall features of the $\kappa(T)$ curves displayed in Figs. 1 and 2 are those found for defect-free insulators: The T^3 behavior at sufficiently low temperatures, due to boundary scattering, and a maximum resulting of normal and Umklapp phonon processes which lead to a $1/T$ dependence above 100 K (see Figs. 1 and 2). We note the following typical features:

(a) We observe a systematic drastic overall decrease of $\kappa(T)$ when the isotopic disorder is increased along the sequence ^{70}Ge(99.99%), ^{70}Ge(96.3%), ^{76}Ge, ^{nat}Ge1, and $^{70/76}$Ge (the latter has the largest isotopic mass variance possible for stable Ge isotopes). The maximum thermal conductivity κ_m of $^{70/76}$Ge is 14 times smaller than that of ^{70}Ge(99.99%), see Table I. The value of κ_m for natural Ge is increased by a factor of ~8 in the ^{70}Ge(99.99%) sample. The increase of κ, however, is only 30% at 300 K. κ_m varies monotonically with the mass variance g, with the exception of sample ^{70}Ge(95.6%). This is shown in Fig. 3 as a graph of

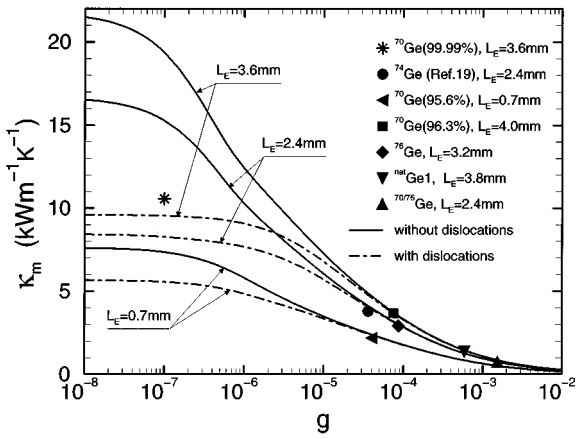

FIG. 3. Maximum of the thermal conductivity κ_m for the Ge samples with different isotopic mass compositions as a function of the mass variance g [defined in Eq. (1)]. The solid lines represent κ_m obtained from ''Model 1'' (see Table II) for three different values of L_E. For the dot-dashed lines, corresponding to ''Model 2,'' dislocation scattering has been taken into consideration to account for the smaller κ_m of ^{70}Ge(99.99%).

κ_m versus g: The symbols represent the experimental data, and the solid and dot-dashed lines κ_m values calculated without and with dislocation scattering, respectively, using the models discussed below (''Model 1'' and ''Model 2'' in Table II). The set of three curves shown (solid and dot-dashed lines) displays the strong dependence of κ_m on the effective phonon mean free path L_E for $T\rightarrow 0$. Sample ^{70}Ge(95.6%) shows a lower κ_m because of the low L_E that results from the additional electronic scattering of the phonons and because of the [110] orientation.

(b) The maximum of $\kappa(T)$ shifts slightly to higher temperatures with increasing isotopic purity (as predicted by theory).[68]

(c) The strong influence of isotopic disorder on κ is clearly displayed over the entire temperature range in which $\kappa(T)$ was measured. All samples tend to reach a T^3 dependence at the lowest temperatures (see T^3 line in Figs. 1 and 2); however, this limit is reached only for the isotopically pure ^{70}Ge(99.99%) sample near and below 4 K. The other samples follow a temperature dependence between T^2 and T^3, depending on the specific surface preparation techniques which will be discussed in Sec. IV D.

(d) The present data for ^{nat}Ge1 and ^{nat}Ge2, displayed in Fig. 2, join smoothly existing measurements for undoped Ge of high crystalline perfection.[7–9] Our samples were subjected to different surface treatments before measuring the thermal conductivity. The results, shown below, will be discussed in Sec. V.

(e) Sample ^{70}Ge(95.6%), doped unintentionally with Ga and having 2×10^{16} holes/cm^3, has κ values approximately four times lower than the other samples in the boundary scattering range. These κ values are in agreement with existing data for p-type Ge[6,9,10] (e.g., with In doped Ge with $p\approx 10^{16}$ cm^{-3}). This decrease in thermal conductivity is attributed to phonon scattering by electronic excitations in the dopants.

IV. ANALYSIS OF THERMAL CONDUCTIVITY VERSUS TEMPERATURE

In view of the high purity ($|N_d\text{-}N_a|<10^{14}$ cm^{-3})—with the exception of sample ^{70}Ge(95.6%)—and crystalline perfection of our samples, we consider only four scattering mechanisms: Normal three-phonon scattering (N), three-phonon Umklapp processes (U), boundary scattering (B), and isotopic mass fluctuations (point defects) (I). The parameters for the two latter mechanisms are taken to be fixed by theory and are therefore *not adjustable*. Dislocation scattering will also be considered.

Point defect scattering from isolated atoms of different mass, either different isotopes or different elements with very similar force constants, is one of the rare cases which for phonons can be calculated analytically without adjustable parameters. Klemens[35] obtained a scattering rate (similar to the familiar Rayleigh scattering of photons)

TABLE II. Overview of thermal conductivity models used in this work and expressions for the scattering rates of the various scattering processes taken into account and the corresponding integration ranges.

			Resistive processes					
Theory	κ	Phonon branch	Boundary τ_B^{-1}	Isotope τ_I^{-1}	Umklapp τ_U^{-1}	Dislocation τ_D^{-1}	Normal τ_N^{-1}	Integr. range (K)
Callaway's model	$\kappa_1+\kappa_2$		$v_B L_E$	$A\omega^4$	$B_1\omega^2T^3$		$B_2\omega^2T^3$	0–375
Holland's model	κ_1	TO	$v_B L_E$	$A\omega^4$			$B_T\omega T^4$	0–101
		TU	$v_B L_E$	$A\omega^4$	$B_{\rm TU}\omega^2/\sinh(x)$			101–118
		L	$v_B L_E$	$A\omega^4$			$B_L\omega^2T^3$	0–333
''Model 1''[a]	$\kappa_1+\kappa_2$	T	$v_B L_E$	$A\omega^4$	$B_{\rm TU}\omega^2Te^{-C_T/T}$		$B_T\omega T^4$	0–118
		L	$v_B L_E$	$A\omega^4$	$B_{\rm LU}\omega^2Te^{-C_L/T}$		$B_L\omega^2T^3$	0–333
''Model 2''[b]	$\kappa_1+\kappa_2$	T	$v_B L_E$	$A\omega^4$	$B_{\rm TU}\omega^2Te^{-C_T/T}$	$B_{\rm TD}\omega$	$B_T\omega T^4$	0–118
		L	$v_B L_E$	$A\omega^4$	$B_{\rm LU}\omega^2Te^{-C_L/T}$	$B_{\rm LD}\omega$	$B_L\omega^2T^3$	0–333

[a]Fit to all samples with the same parameters, without including dislocation scattering.

[b]Like footnote ''a'' but including dislocation scattering.

$$\tau_I^{-1} = A\omega^4, \quad A = \frac{gV}{4\pi v_B^3}, \tag{2}$$

with the constant A containing the mass variance g, the volume per atom V, and an averaged sound velocity v_B. Equation (2) corresponds to a Debye-like phonon density of states $D(\omega) \sim \omega^2$ which, although only approximate,[69] will be shown to suffice to account for the global experimental results.

Boundary scattering leads at low temperatures to a T^3 dependence of κ, the prefactor being determined by the geometrical size of the sample and the details of the surface. The scattering rate can be written:

$$\tau_B^{-1} = \frac{v_B}{L_E}, \tag{3}$$

where L_E represents an *effective phonon mean free path*, of the order of the cross-sectional dimensions, that includes effects resulting from sample size, geometry, aspect ratio, phonon focusing, specular/diffuse reflection at the surface, etc. It is important to determine the value of L_E as precisely as possible from the low temperature data for two reasons: (a) L_E is later introduced in the theories as a fixed, nonadjustable length, which influences the $\kappa(T)$ curves in the entire temperature range, (b) in order to detect and interpret effects of specularity and phonon focusing.

In the following we analyze the experimental data in the framework of the widely used scattering theory of $\kappa(T)$ formulated by Callaway[16] and the modifications introduced by Holland.[19] We found it necessary to develop a modification of Callaway's formulation in order to represent the $\kappa(T)$ curves by *a single set of fitting parameters valid for all samples*, independent of their isotopic composition. We also describe the theoretical background used for the analysis of $\kappa(T)$ in surface-treated samples. We have determined the fit parameters B_i by a nonlinear regression procedure for each sample. Then a single optimized parameter set, the same for all samples, was found by systematic variation of the B_i's in order to achieve the best representation of the experimental values for all samples over the entire temperature range with the given theory, whereby preference was given to a good fit in the region near κ_m.

A. Data analysis with Callaway's model

This model assumes[16] (a) a Debye-like phonon spectrum,[70] with no anisotropies or particular structures in the phonon density of states, i.e., no distinction of polarization (between longitudinal and transverse phonons); (b) one averaged sound velocity v_B; (c) diffuse scattering at the surface of the sample [see Eq. (3)]; (d) normal three-phonon processes, included with a relaxation rate $\tau_N^{-1} = B_2\omega^2 T^3$, which should only be valid for low-frequency longitudinal phonons;[14] (e) three-phonon Umklapp processes assumed to have a relaxation rate like that of N processes $\tau_U^{-1} = B_1\omega^2 T^3$;[15] (f) that all phonon scattering processes can be represented by relaxation times depending on frequency and temperature; and (g) the additivity of the reciprocal relaxation times for independent scattering processes. The total thermal conductivity κ can then be written as[16,36,53]

$$\kappa = \kappa_1 + \kappa_2, \tag{4}$$

where κ_1 and κ_2 are defined by

$$\kappa_1 = CT^3 \int_0^{\theta/T} \tau_C(x) J(x)\, dx, \tag{5}$$

$$\kappa_2 = CT^3 \frac{\left[\int_0^{\theta/T} \frac{\tau_C(x)}{\tau_N(x)} J(x)\, dx\right]^2}{\int_0^{\theta/T} \frac{\tau_C(x)}{\tau_N(x)\tau_R(x)} J(x)\, dx} = CT^3(\beta I), \tag{6}$$

with

$$\beta = \frac{\int_0^{\theta/T} \frac{\tau_C(x)}{\tau_N(x)} J(x)\, dx}{\int_0^{\theta/T} \frac{\tau_C(x)}{\tau_N(x)\tau_R(x)} J(x)\, dx}, \quad I = \int_0^{\theta/T} \frac{\tau_C(x)}{\tau_N(x)} J(x)\, dx,$$

and

$$J(x) = \frac{x^4 e^x}{(e^x - 1)^2}, \quad \frac{1}{\tau_C(x)} = \frac{1}{\tau_N(x)} + \frac{1}{\tau_R(x)},$$

$$x = \frac{\hbar\omega}{k_B T}, \quad m = \frac{k_B}{\hbar}, \quad C = \frac{k_B m^3}{2\pi^2 v_B} \tag{7}$$

[see also Eqs. (19) to (21) in Ref. 16].

In Eq. (7) k_B is Boltzmann's constant, $\hbar$ is Planck's constant, and $\tau_N(\tau_R)$ denotes the relaxation time of N processes (resistive processes). The corresponding combined relaxation rate τ_C^{-1} can be written as the sum of the normal, nonresistive rate (N) and the resistive rate (R): $(1/\tau_C) = (1/\tau_N) + (1/\tau_R)$. In the Callaway formulation, in contrast to the earlier models of Klemens[15] and Ziman,[61] all resistive scattering probabilities are taken to be additive $(1/\tau_R) = \Sigma_i (1/\tau_i)$ [here τ_i represents the isotopic (τ_I), the boundary (τ_B), and the Umklapp (τ_U) scattering times], i.e., the corresponding scattering mechanisms are assumed to be independent. Although N processes do not contribute directly to the thermal resistance, they are crucial in spreading out the influence of the other resistive processes to the entire phonon spectrum.

The κ_2 term is not only a correction term to κ_1 (as sometimes stated in the literature[16,17]) but is essential to counteract the effect of treating N processes in τ_C as if they were entirely resistive. Consequently, κ_2 is a non-negligible part of Callaway's theory. Our calculations reveal that the contribution of κ_2 remains below 1% for the samples studied, with the exception of the pure ^{70}Ge(99.99%) crystal for which κ_2 increases to 20% of the total thermal conductivity. The magnitude of κ_2 is essentially controlled by the concentration of point defects. In the majority of cases of physical interest resistive scattering dominates ($\tau_N \gg \tau_R \Rightarrow \tau_C \approx \tau_R \Rightarrow \kappa_2 \ll \kappa_1$) and only κ_1 is important. Therefore, in the literature, usually only the κ_1 term is included. (This is also the case in Callaway's original calculations;[16,17] after having introduced κ_1 *and* κ_2, κ_2 was assumed to be small and therefore neglected and only κ_1 was kept.) However, when N processes

become comparable to the resistive processes ($\tau_N \approx \tau_R$), e.g., in very pure, defect-free (i.e., isotopically pure) samples, the κ_2 integrals contribute significantly to the total thermal conductivity.[22,23,36,40,53] A remarkable feature in the context of isotopic scattering is the strong dependence of κ_2 on even small concentrations of different isotopes (see Ref. 36 for LiF). Thus, in isotopically pure samples, normal three-phonon scattering rather than Umklapp processes determine the phonon mean free path.

Using the Callaway model in its original form, i.e., keeping both κ_1 *and* κ_2, we adjusted *two free parameters* (B_1, B_2) in the combination of the four scattering mechanisms considered, with the scattering rates for isotopic and boundary scattering fixed to the values given in Eqs. (2) and (3) ($V = 22.6 \times 10^{-30}$ m^3, $v_B = 3500$ m/s, g and L_E taken from Table I). In this manner, an acceptable representation of all the data was achieved but *only below about 30* K. Moreover, the adjustable coefficients obtained were not the same for the various samples. As a typical example, the fit to the data for natural Ge with Callaway's theory is shown in Fig. 2 (dashed line), calculated for $B_1 = B_2 = 2.6 \times 10^{-23}$ s/K^3. The convexity of the calculated thermal conductivity above the maximum, describing a steeper decrease of $\kappa(T)$ with increasing temperature than found experimentally, cannot be removed by changing the parameters. The reason can be traced to an underestimation of the U processes in that model. Instead of using an exponential function for the Umklapp scattering probability, as proposed in the literature,[12,14,15,71,72] the N processes, as well as the U processes, are represented by the same temperature and frequency dependences $B_{1/2}\omega^2 T^3$. The prefactors B_1 and B_2 are thus indistinguishable in Callaway's theory.

B. Data analysis with Holland's model ($\kappa_2 = 0$)

In the next step, we apply Holland's theory,[19] who extended the Callaway theory to include explicitly the thermal conductivity by both transverse and longitudinal phonons, under the assumption $\kappa_2 = 0$:

(a) Since the variation of the phonon relaxation times with frequency and temperature strongly depend on the actual phonon branch and its dispersion, the contributions to the thermal conductivity by the two kinds of differently polarized phonons (transverse and longitudinal), are considered separately while normal processes are taken into account for the class of crystal at hand, as suggested by Herring.[14] For an overview of the frequency and temperature dependences of the different scattering processes we refer to Table II (and to Table I in Ref. 19).

(b) A more realistic representation of the very dispersive transverse acoustic modes of Ge is used[73] (see below). It involves splitting the range of integration in two parts, a low and a high frequency range with different temperature and frequency dependences. (The complex behavior of the density of phonon states of Ge is shown in Figs. 2 and 3 of Ref. 73.) Notice that the frequency spectrum of the T1 phonons, the lowest TA branch, has a very high peak at 2.4 THz, whereas the longitudinal acoustic modes become important only at frequencies higher than about 3.7 THz.

The four scattering mechanisms assumed for the analysis with Holland's model are chosen to have the following temperature and frequency dependence (see also Table II):

$$\tau_I^{-1} = A\omega^4, \tag{8}$$

$$\tau_B^{-1} = \frac{v_B}{L_E}, \tag{9}$$

$$\tau_{\mathrm{TO}}^{-1} = B_T \omega T^4 \quad \text{for} \quad 0 \leqslant \omega < \omega_1, \tag{10}$$

$$\tau_L^{-1} = B_L \omega^2 T^3 \quad \text{for} \quad 0 \leqslant \omega \leqslant \omega_3, \tag{11}$$

$$\tau_{\mathrm{TU}}^{-1} = \frac{B_{\mathrm{TU}}\omega^2}{\sinh(x)} \quad \text{for} \quad \omega_1 \leqslant \omega \leqslant \omega_2, \tag{12}$$

$$\tau_{\mathrm{TU}}^{-1} = 0 \quad \text{for} \quad \omega < \omega_1,$$

where $x = (\hbar\omega/k_B T)$ and $T(L)$ represent transverse (longitudinal) acoustic phonons. We redefined an average of the transverse ($v_T = 3550$ m/s) and longitudinal ($v_T = 2460$ m/s) velocities:

$$v_B = \left[\frac{1}{3}\left(\frac{2}{v_T} + \frac{1}{v_L}\right)\right]^{-1} = 3900 \text{ m/s}. \tag{13}$$

Isotopic (point defect) scattering [Eqs. (2),(8)] gives rise to a temperature independent relaxation time with an ω^4 dependence. We use $A = g 3.03 \times 10^{-41}$ s^3, as obtained for $v_B = 3900$ m/s and the values of g listed in Table I. At higher frequencies, where the acoustic dispersion becomes appreciable, the scattering rate is expected to increase with frequency faster than ω^4, because the density of states grows more rapidly[69] than ω^2. However, we have not found it necessary to include this effect within the accuracy of our analysis.

Boundary scattering [Eqs. (3),(9)] should be dominant for our Ge samples below 8 K. The values of L_E used for the calculations are given in Table I. We have again used $v_B = 3900$ m/s and implicitly included in L_E all effects which, in addition to the sample size, may influence $\kappa(T)$ in the boundary scattering region, such as the shape of the cross section and the aspect ratio of the sample, specular phonon reflection, phonon focusing, etc. The use of an average sound velocity v_B instead of the velocities v_T and v_L, which depend on crystallographic direction, may be an oversimplification. We have checked, however, that this simplification does not appreciably change our results. A justification for using the average v_B in the boundary and isotopic relaxation rates is given in Ref. 19.

Normal phonon scattering (three-phonon processes) has been discussed by Herring,[14] Klemens,[35] and Ziman.[61] Herring gave the most comprehensive treatment for complicated dispersion relations. Here, we use his expressions for the corresponding low temperature transverse and longitudinal relaxation rates [see Eqs. (10),(11)]. The discrimination between T and L modes is indispensable in order to improve data fitting. At high temperatures the N-scattering rates are negligible because of the dominant U processes.[19]

Umklapp processes [Eq. (12)] are taken into account for phonon frequencies between $\omega_1 = 1.34$ THz and $\omega_2 = 1.57$ THz, corresponding to Debye temperatures of 101 K and 118 K, the range of the highest TA frequencies of Ge.[73] We

TABLE III. Single parameter set (valid for all samples studied) based on Holland's model and on all other models used to represent the temperature dependence of the thermal conductivity κ.

Theory	κ	Normal		Umklapp				Dislocation	
		$B_T\left(\frac{1}{K^4}\right)$	$B_L\left(\frac{s}{K^3}\right)$	B_{TU} (s)	B_{LU} (s)	C_T (K)	C_L (K)	B_{TD}	B_{LD}
Holland's model[a]	κ_1	1.0×10^{-11}	6.9×10^{-24}	5.0×10^{-18}					
Holland's model[b]	κ_1	1.5×10^{-11}	9.0×10^{-24}	4.5×10^{-18}					
''Model 1''[c]	$\kappa_1+\kappa_2$	2×10^{-13}	2×10^{-21}	1×10^{-19}	5×10^{-19}	55	180		
''Model 2''[d]	$\kappa_1+\kappa_2$	2×10^{-13}	2×10^{-21}	1×10^{-19}	5×10^{-19}	55	180	1×10^{-8}	3×10^{-7}

[a]Fit, performed by Holland (Ref. 19), includes only κ_1 for the data of $^{\mathrm{nat}}$Ge given in Refs. 4,83.
[b]Like footnote a but our fit, leading to slightly different parameters than those given by Holland (Ref. 19), because of having fitted all our samples.
[c]Fit to all samples with the same parameters, but without including dislocation scattering.
[d]Like footnote c but including dislocation scattering.

actually approximate the acoustic branch of Ge by a linear range below ω_1 and a frequency independent range $\omega_1<\omega<\omega_2$.

The thermal conductivity is calculated using only the Callaway integral κ_1 which, following Holland [Eqs. (9)–(13) in Ref. 19], has been separated into TA and LA contributions κ_T and κ_L. The term κ_T splits up into the contribution of N processes κ_{TO} and that of U processes κ_{TU} (note the limits of integration):

$$\kappa=\kappa_T+\kappa_L=\kappa_{\mathrm{TO}}+\kappa_{\mathrm{TU}}+\kappa_L, \tag{14}$$

with

$$\kappa_{\mathrm{TO}}=\frac{2}{3}H_{\mathrm{TO}}T^3\int_0^{\theta_1/T}\tau_C^{\mathrm{TO}}(x)J(x)dx, \tag{15}$$

$$\kappa_{\mathrm{TU}}=\frac{2}{3}H_{\mathrm{TU}}T^3\int_{\theta_1/T}^{\theta_2/T}\tau_C^{\mathrm{TU}}(x)J(x)dx, \tag{16}$$

$$\kappa_L=\frac{1}{3}H_LT^3\int_0^{\theta_3/T}\tau_C^{L}(x)J(x)dx, \tag{17}$$

where

$$\tau_C^{\mathrm{TO}}(x)=\left(\frac{v_B}{L_E}+Am^4x^4T^4+B_TmxT^5\right)^{-1},$$

$$\tau_C^{\mathrm{TU}}(x)=\left(\frac{v_B}{L_E}+Am^4x^4T^4+\frac{B_{\mathrm{TU}}m^2x^2T^2}{\sinh(x)}\right)^{-1},$$

$$\tau_C^{L}(x)=\left(\frac{v_B}{L_E}+Am^4x^4T^4+B_Lm^2x^2T^5\right)^{-1},$$

and

$$H_i=\frac{k_Bm^3}{2\pi^2v_i},\quad m=\frac{k_B}{\hbar}. \tag{18}$$

In each of the three integrals the constants H_i contain the corresponding sound velocity v_i: $v_{\mathrm{TO}}=3550$ m/s (in H_{TO}), $v_L=4920$ m/s, and $v_{\mathrm{TU}}=1300$ m/s, respectively. We emphasize that U processes are neglected in Eq. (15) because they should not contribute below ω_1 ($\theta_1=101$ K). The term for N processes was omitted from Eq. (16) since it should be relatively small above ω_1. Both assumptions have been checked to be quantitatively justified.[19] Nevertheless, the integral formulation causes each of the scattering mechanisms to be operative over a large temperature interval. Thus, the effect of varying one of the coefficients always induces modifications in the influence of the other coefficients on the thermal conductivity.

The *three free adjustable coefficients—B_T, B_L,* and B_{TU}—have been obtained by linear regression, as outlined before. The isotopic and boundary scattering rates were fixed by Eqs. (2) and (3), the corresponding mass variance g, the effective mean free path L_E, and the sound velocity v_B, respectively. With this model we have been able to obtain a good representation of the *thermal conductivity of all samples* studied using a *unique set of parameters* in the temperature range 2 K to 200 K. The agreement between experimental data and fitted curves is rather good ($\pm5\%$), as exemplified by the solid line in Fig. 2 for natural Ge. The unique set of parameters obtained from our fits is listed in Table III together with Holland's original set of parameters for natural Ge. Obviously, our set of unique fit parameters, valid for all samples, does not represent the best possible fit for an *individual* sample. For each sample, a better fit can be found with parameters specific to it. However, no physical meaning can be attributed to these parameters.

C. Data analysis with the modified Callaway/Holland model for $\kappa_2\neq0$

As outlined above, it is unreasonable to suppress the κ_2 term in Callaway's theory when normal scattering processes are included. This makes questionable the otherwise good fits obtained in Sec. IV B for $\kappa_2=0$. In the κ_1 term N processes are implicitly treated as entirely resistive. Therefore, whenever N processes are important, one should perform the calculation of $\kappa(T)$ with the ''full'' Callaway form $\kappa=\kappa_1+\kappa_2$ in order to account for the nonresistive nature of the N processes. The suppression of the κ_2 term is only acceptable if resistive scattering processes dominate, which is usually not the case for isotopically pure and defect-free samples. Curve fitting with $\kappa_1+\kappa_2$, however, is numerically

much more difficult (in view of poor convergence of the integrals involved) than treating only κ_1.

We thus attempted several modifications, involving changes of the scattering processes in the models described by Callaway and Holland, suggested by scrutinizing their basic assumptions. Table II lists the temperature and frequency dependences of the various scattering mechanisms used in the different models. The mechanisms finally applied, which led to an improved description of $\kappa(T)$ for all samples, are indicated in Table II as ''Model 1'' and ''Model 2.''

The present study and the corresponding results for diamond[22,23,39,40,74] show that *the separation of the phonon modes into transverse and longitudinal* results in improved fits with a single set of parameters for the whole series of isotopically different samples available. This fact is supported by the suggestion that, up to room temperature, the transverse phonon branches yield the dominant contribution to $\kappa(T)$. The separation into T and L modes can be performed in different ways:

(a) *Original Holland model*:[19] The κ_1 term is split into transverse $(2T)$ and longitudinal $(1L)$ modes, whereas the transverse mode is again split in 2TO and 2TU and therefore three free adjustable parameters (B_T, B_{TU}, and B_L) are used. This model yields reasonable results, but is unacceptable on physical grounds since it assumes $\kappa_2=0$.

(b) *Modified original Holland model*: The splitting of the original Holland model in transverse (2TO, 2TU) and longitudinal $(1L)$ branches was used while keeping Callaway's κ_2 term. Disappointingly, no reasonable fits could be found. The calculated thermal conductivity leads to unreasonably high values of κ (above 8 K–10 K) that exceed the experimental values above 100 K by orders of magnitude. The ratio of the integrals [the β term in κ_2, see Eq. (6)] is responsible for this ''mishap.'' Even the addition of longitudinal $(0\leqslant\omega<\omega_1)$ or transverse $(0\leqslant\omega\leqslant\omega_3)$ Umklapp processes, does not remedy this problem.

(c) *Modified Callaway/Holland model*: Both terms κ_1 and κ_2 are kept and the distinction into transverse $(2T)$ and longitudinal $(1L)$ modes is used in analogy to Holland's calculations. This procedure introduces, in contrast to model (a), one more free-adjustable prefactor B_{LU} representing longitudinal Umklapp processes. In this model longitudinal U processes are decisive for ensuring the decrease of $\kappa(T)$ at higher temperatures and it is essential for the fits to the data as pointed out earlier.[69,75,76] In conclusion, N processes and also U processes involving transverse and also longitudinal phonons are needed for the calculation of the total thermal conductivity $\kappa_1+\kappa_2$.

Some of the arguments given by Holland to justify neglecting longitudinal U processes are not expected to hold at higher temperatures ($T>100$ K); all fitting attempts we made indicate that *longitudinal Umklapp processes are indispensable*. The splitting of the transverse acoustic branch in two frequency ranges, however, seems to be unnecessary. Moreover, better results[12,14,15] were found using the exponential function ($B_{iU}\exp^{-C_i/T}$, with $i=T,L$) for all Umklapp scattering processes instead of the $\sinh(x)$ dependence, proposed by Holland.[19]

We also tried an approach suggested by Berman[53] for calculating the $\kappa(T)$ of pure samples, in cases when N processes are dominant and resistive processes are present. Then τ_C is mainly determined by τ_N, this means $\tau_C\approx\tau_N$, consequently, $\kappa_2\gg\kappa_1$ and therefore κ_2 alone should describe the total thermal conductivity. This procedure works for the ^{70}Ge(99.99%) sample, although in the region of κ_m the agreement between the calculations and the measured data is not as good as achieved with Holland's model (the calculated values are too large). The deviation between measurement and calculations increases with increasing g. With this assumptions also Olson *et al.*[22] tried to fit their data of natural and enriched diamond, but this led to an incorrect temperature dependence for one or the other specimens.

The final form chosen to fit the experimental $\kappa(T)$ data (''Model 1'') is very similar to the formalism applied by Wei *et al.*[23] to describe the thermal conductivity of isotopically modified diamond. We start with the Callaway integrals, $\kappa=\kappa_1+\kappa_2$, Eq. (4), using two transverse $(2T)$ and one longitudinal (L) branch and integrate up to 118 K for the transverse and up to 333 K for the longitudinal modes, with N and U processes for each mode. The relevant temperature and frequency dependences are listed in Table II (''Model 1''). The resulting values of the six fitting coefficients, B_T, B_L (N processes), B_{TU}, C_T, B_{LU}, and C_L (U processes) are given in Table III and constitute *a single set of parameters* which describes reasonably well the thermal conductivity of all isotopically modified Ge samples (including also data from the literature) in the temperature range between 2 K and 300 K. The experimental data for all investigated Ge samples, and the $\kappa(T)$ curves calculated with this parameter set are shown in Fig. 4. This figure probably contains the most comprehensive description of thermal conductivity as a function of isotopic composition ever obtained. The agreement between the experiments and the model calculations is good. Deviations between calculated and experimental curves occur above 200 K for all samples, and near κ_m especially for the isotopically pure ^{70}Ge(99.99%) [Fig. 4(a)]. The discrepancies above 200 K may be either due to systematic experimental errors (e.g., insufficient temperature control of the heat shield) or to shortcomings of the theoretical model (it may be that the use of different temperature and frequency dependences for the considered scattering mechanisms can solve this problem).

The disagreement for the ^{70}Ge(99.99%) curve [Fig. 4(a)] in the region of the maximum, however, must be explained by introducing other scattering mechanisms. A plausible mechanism active in the range below 50 K is scattering by dislocations (it is hard to pinpoint other scattering processes acting in this temperature range). Theories for phonon scattering from single dislocations predict a linear frequency dependence ($\tau_D^{-1}\sim\omega$).[2,13,35,53] We therefore added to ''Model 1,'' used to perform the curve fitting shown in Fig. 4, terms for the scattering of the transverse and longitudinal phonons by dislocations: $\tau_D^{-1}=B_{iD}\omega$, $i=T,L$. The fitted values of the two new coefficients B_{TD} and B_{LD}, are listed in Table III as ''Model 2'' (the other six parameters were left the same as in ''Model 1'').

A comparison of the fitted curves, *with* and *without* dislocation scattering, is given in Fig. 5 for ^{70}Ge(99.99%) (a) and $^{70/76}$Ge (b). The thermal conductivity of the isotopically very pure sample ^{70}Ge(99.99%) is much better represented with [dot-dashed line in Fig. 5(a), ''Model 2''] than without

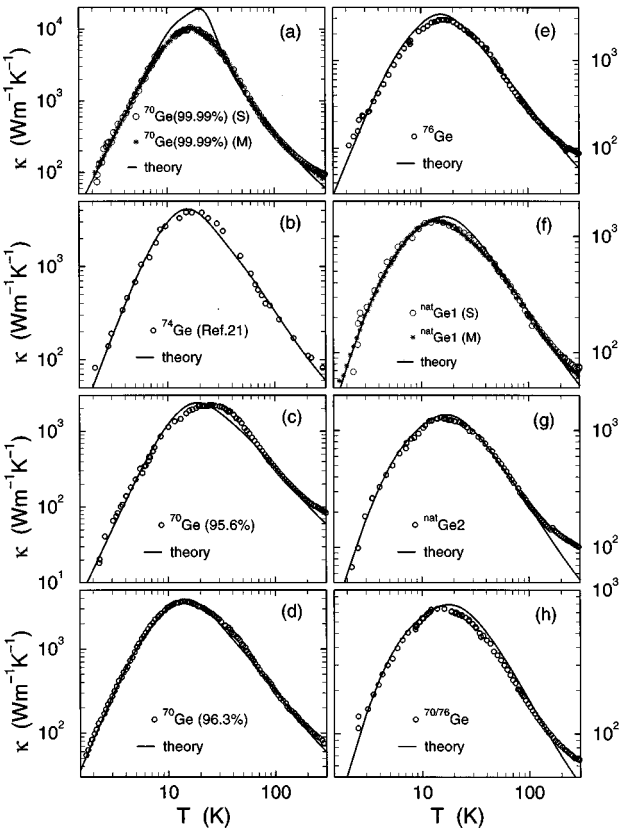

FIG. 4. Thermal conductivity $\kappa(T)$ measured for all Ge crystals under consideration, with mass variances g between 1.0×10^{-7} (a) and 1.5×10^{-3} (h), together with the calculated thermal conductivity curves based on ''Model 1'' (Tables II and III) with the parameter set $B_T=2\times10^{-13}$ 1/K^4, $B_L=2\times10^{-21}$s/K^3, $B_{\rm TU}=1\times10^{-19}$ s, $C_T=55$ K, $B_{\rm LU}=5\times10^{-19}$ s, $C_L=180$ K, and L_E and g taken from Table I.

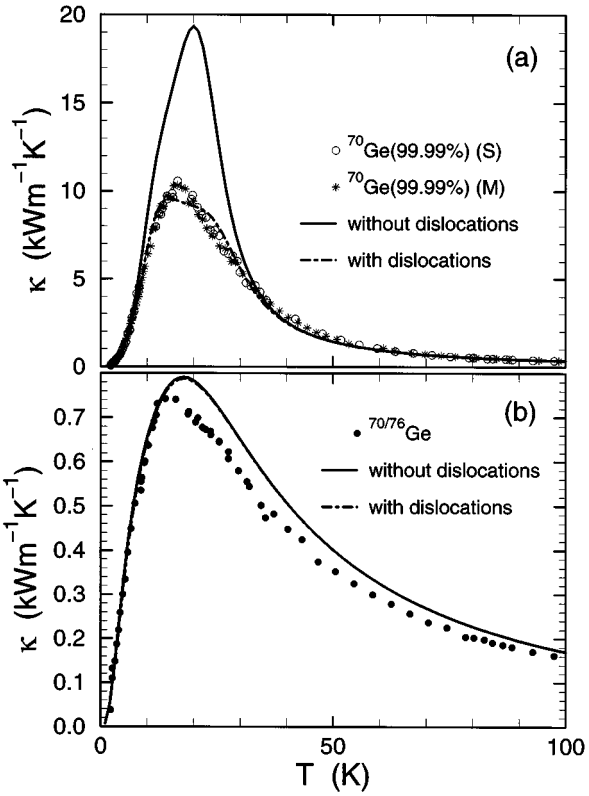

FIG. 5. Thermal conductivity calculated with ''Model 1'' and ''Model 2'' (Table II), for ^{70}Ge(99.99%) (a) and $^{70/76}$Ge (b). The solid lines show the results obtained without dislocation scattering, whereas for the dot-dashed lines dislocations were taken into account. For $^{70/76}$Ge the full and the dot-dashed lines are nearly the same.

dislocation scattering [solid line in Fig. 5(a), ''Model 1''], whereas the differences between ''Model 1'' and ''Model 2'' are indistinguishable for the case of sample $^{70/76}$Ge [Fig. 5(b)] and for all other isotopic compositions. The possible presence of a small amount of dislocations, comparable to that seen in ^{70}Ge(99.99%), affects the calculated $\kappa(T)$ only when the sample is isotopically pure (see discussion in Sec. V).

In conclusion, the modified Callaway/Holland integrals seem to provide a physically sound and accurate formulation for the representation of the temperature and isotopic dependences of the thermal conductivity of germanium and diamond. We note that for diamond[23,40] $\tau_N^{-1}\sim\omega T^3$ has been applied instead of $\tau_N^{-1}\sim\omega T^4$ (transverse) and $\tau_N^{-1}\sim\omega^2T^3$ (longitudinal) as suggested by Herring.[14] In view of the ratio of the Debye temperatures of germanium and diamond ($\theta_T^{\rm Ge}=118$ K and $\theta_L^{\rm Ge}=333$ K, $\theta_T^{\rm C}\approx2150$ K and $\theta_L^{\rm C}\approx2940$ K) and the position of κ_m on the temperature scale ($\kappa_m^{\rm Ge}\approx15$ K, $\kappa_m^{\rm C}\approx100$ K), the normalized fitting range for our Ge samples is about six times larger than that for diamond.

D. Thermal conductivity in the boundary scattering region

1. Surface treatment

Crystallographic orientation and surface treatment, together with geometrical dimensions, determine the thermal conductivity in the low temperature range. Three samples were subjected to surface treatments before measuring again their thermal conductivity: The isotopically very pure ^{70}Ge(99.99%), ^{70}Ge(95.6%), and ^{nat}Ge1. The corresponding experimental results are shown in Figs. 6 and 7. The thermal conductivity of ^{nat}Ge1 is successively improved below 30 K when the sample, initially ground with 20 μm diamond powder, is then ground with 3 μm diamond powder and, in a last step, is polish etched with SYTON.[77] We observe a very small increase in $\kappa(T)$ detectable only at the lowest temperatures, when a sample ground with 20 μm diamond powder is ground with 3 μm diamond powder (see Fig. 6). However, a significant increase in $\kappa(T)$ (a factor of 2.5 at 3 K) takes place, after polishing with SYTON. Polish etching with CP4 (Ref. 78) after the SYTON treatment reduces $\kappa(T)$ at 3 K by about 30%. This can be taken as a signature of surface deterioration.

The surface of sample ^{70}Ge(99.99%) was also polished with SYTON and measured in Stuttgart (S) as well as in Moscow (M): Nearly identical $\kappa(T)$ curves were obtained. The enhancement at 3 K after the SYTON treatment also amounts to a factor of 2 (see Fig. 7). It can be attributed to increasing specular reflection as a result of improved surface quality. The SYTON treatment thus seems to yield the best Ge surfaces, as revealed by the high values of κ. Although CP4 also improves the quality of ground surfaces, it is less effective than SYTON. This is supported by measurements of sample ^{70}Ge(95.6%) (see Fig. 7) which was first measured

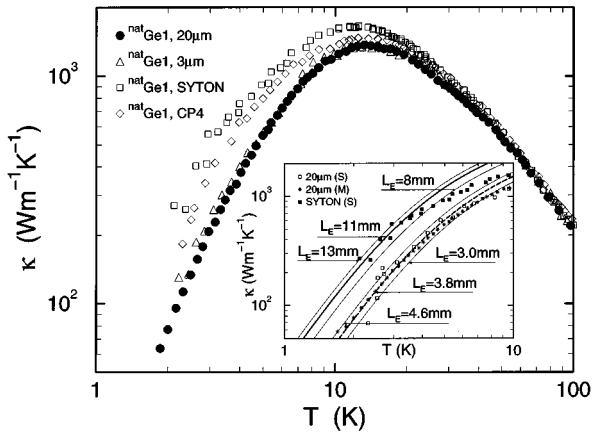

FIG. 6. Influence of surface preparation (diamond powder slurry, SYTON and CP4) on the thermal conductivity of sample ^{nat}Ge1 in the low temperature range. The heat conductivities for two different surface treatments (20 μm diamond and SYTON) are shown in the inset together with calculations for various values of L_E, taking into account only boundary and isotope scattering.

after grinding with 20 μm diamond powder and remeasured after polish etching with CP4. This procedure increased κ by a factor of 1.5 at 3 K, i.e., less than the enhancement expected for SYTON polishing. The same result is obtained when ^{nat}Ge1 was polish etched with CP4 after the SYTON treatment (Fig. 6).

2. Determination of L_E

A precise determination of L_E is crucial for correctly describing the $\kappa(T)$ curve in our full temperature range. Therefore two methods have been used to extract L_E from the experimental data. The first one[36] consists of plotting $\kappa(T)/T^3$ versus T so as to accentuate the behavior of $\kappa(T)$ in the region of pure boundary scattering. This procedure is exemplified in the inset of Fig. 7 where such plots are shown

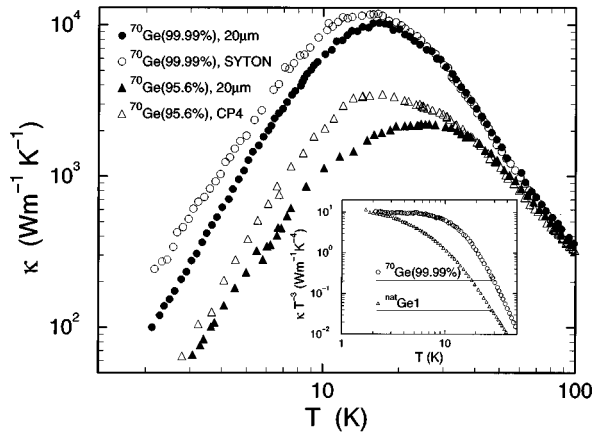

FIG. 7. Thermal conductivity of isotopically pure Ge, samples ^{70}Ge(99.99%) and ^{70}Ge(95.6%), with surfaces ground with 20 μm diamond powder, and after polish etching with either SYTON or CP4. The inset shows the measured κ/T^3 vs T for ^{70}Ge(99.99%) and for ^{nat}Ge1, used for the determination of the phonon mean free path L_E in the low temperature, boundary scattering regime.

for two samples, ^{70}Ge(99.99%) and ^{nat}Ge1. For ^{70}Ge(99.99%) a value of $L_E=(3.0\pm0.2)$mm is found from the flat portion of the $\kappa(T)/T^3$ curve. This method is not as accurate for all the other samples, as shown for ^{nat}Ge1 in the same inset: The range of pure boundary scattering is also approached for $T\rightarrow 0$ but a flat region is not reached in the investigated temperature range, a fact which increases the error in the determination of L_E. Therefore we used a second, more reliable method, where the parameter L_E is determined from the measured thermal conductivity data below 8 K using a sequence of curves calculated for various values of L_E, taking into account two mechanisms, boundary *and* isotopic scattering (the other mechanisms are negligible below 10 K). The implementations of this method is illustrated in the inset of Fig. 6 for ^{nat}Ge1 with differently prepared surfaces. We deduce for the as-ground sample $L_E=(3.8\pm0.4)$ mm, a value slightly larger than that evaluated with the first method (inset, Fig. 7). For each sample, the value of L_E was determined from the data below 8 K according to these two procedures. The effective phonon mean free paths obtained from calculations of $\kappa(T)$ including boundary and isotopic scattering are given in Tables I and IV.

Boundary-limited thermal conductivity, as found in pure dielectric crystals in the range of liquid helium, results from scattering of phonons at the crystal surface.[50] The thermal conductivity is then proportional to T^3 and depends linearly on the sample dimensions when the surface scattering is strictly diffuse.[50,53] In such cases, the expression for the thermal conductivity approaches

$$\kappa=\frac{1}{3}C_V v_B L_C, \tag{19}$$

where C_V represents the heat capacity, v_B the average sound velocity, and L_C the so-called ''Casimir length.'' For a circular cylinder with radius R, this length is equal to $L_C=2R$ while for a square or rectangular cross section with side lengths a and b, $L_C=1.12L_G$, and $L_G=(ab)^{0.5}$. The relevant relaxation rate as a function of geometrical sample size thus becomes [in analogy to Eq. (3)]:

$$\frac{1}{\tau_B}=\frac{v_i}{L_C}=\frac{v_i}{1.12L_G}, \tag{20}$$

where i indicates the transverse and longitudinal modes. Table IV lists the parameters L_C and L_G for the samples under study, as well as the values of the sample widths a and b, length l, and cross section ab. Deviations from the T^3 behavior are likely to occur for several reasons.

(a) The effect of *finite sample length*, resulting in a decrease of κ, can be approximated by defining an effective mean free path $(1/L_E)=(1/L_C)+(1/l)$, where l denotes the length of the sample in the direction of the heat flow.[39,51–56] In this case the relaxation rate for boundary scattering τ_B^{-1} can be written in the general form, including the size correction discussed before:

$$\frac{1}{\tau_B}(l)=\frac{v_i}{L_E}=v_i\left(\frac{1}{L_C}+\frac{1}{l}\right). \tag{21}$$

TABLE IV. Sample parameters relevant for the determination of the low temperature limited mean free path L_E and the specular reflection parameter P. η_{SC} is calculated like η (Ref. 59), but including the size correction Eq. (22) with (24). Some of the samples had been subjected to different surface treatments.

			Geometry				Char. lengths							
Sample	g (10^{-5})	O	a (mm)	b (mm)	l (mm)	ab (mm^2)	L_G (mm)	L_C (mm)	L_E (mm)	η_E (Å)	η_{SC} (Å)	η (Å)	P	Sample treatment
^{70}Ge(99.99%)	0.01	100	2.20	2.50	44.5	5.50	2.35	2.63	3.6	15	45	160	0.19	20 μm
			2.13	2.40	44.5	5.11	2.26	2.53	7.5	8	20	80	0.50	SYTON
^{74}Ge	3.6	100	1.57	1.57	12.0	2.46	1.57	1.76	2.4	12	30	130	0.18	
^{70}Ge(95.6%)	4.0	110	1.25	1.49	14.0	1.86	1.36	1.53	0.70					
^{70}Ge(96.3%)	7.57		2.50	2.50	28.0	6.25	2.50	2.80	4.0	22	45	150	0.20	
^{76}Ge	8.7	100	1.27	2.54	35.0	3.23	1.80	2.01	3.2	18	45	120	0.15	
^{nat}Ge1	58.7	100	2.46	2.50	29.4	6.15	2.48	2.78	3.8	23	65	150	0.13	20 μm
			2.41	2.44	29.2	5.88	2.42	2.72	4.0	23	65	130	0.15	3 μm
			2.35	2.40	29.0	5.64	2.37	2.66	11	10	20	$<$70	0.68	SYTON
			2.30	2.33	29.0	5.36	2.31	2.59	7.0	12	25	65	0.55	CP4
^{nat}Ge2	58.7	100	1.30	1.30	15.0	1.69	1.30	1.46	3.0	13	30	80	0.28	
^{nat}GeI		100	1.26	1.26	39.5	1.59	1.26	1.41	2.2	35	90	170	0.18	sandblast
^{nat}GeII	58.7	100	1.32	1.32	40.0	1.74	1.32	1.48	4.2	20	45	90	0.48	1 μm
^{nat}GeIII		100	1.17	1.17	40.6	1.37	1.17	1.31	7.5	13	28	60	0.75	LUSTROX
$^{70/76}$Ge	153	110	2.02	2.00	23.0	4.04	2.01	2.25	2.4	30	90	200	0.06	

Note that we neglected the small effect of details of the sample thermometer arrangement (e.g., the position of the thermocouples, see also Sec. II), which is discussed in Ref. 79.

(b) *Partial specularity* of the phonon scattering at the sample surfaces can decrease the effect of boundary scattering. The sample then appears to have larger dimensions than it actually has.[39,43,52–56,59–62] The relaxation rate is then rewritten in the form

$$\frac{1}{\tau_B}(l,P)=v_i\left(\frac{1}{L_C}\frac{(1-P)}{(1+P)}+\frac{1}{l}\right). \tag{22}$$

The expression for the ''effective'' mean free path L_E (or the relaxation rate τ_B^{-1}), used for the description of the $\kappa(T)$ curves, may encompass various effects and has the form

$$L_E(l,P)=\left(\frac{1}{L_C}\frac{(1-P)}{(1+P)}+\frac{1}{l}\right)^{-1}. \tag{23}$$

In principle, Eq. (23) enables us to calculate P from the sample geometry (Casimir length) and from the effective mean free path L_E, determined from the low temperature range in which $\kappa(T)\sim T^3$. P varies from zero to one. Whenever $P>0$, partial specular reflection occurs (e.g., $P=0.5$ corresponds to a phonon mean free path of three times the geometrical Casimir length with an average of two boundary reflections; $P=0.75$ yields $\sim$sevenfold length and sixfold reflexions). The determination of P using Eq. (23) is hampered by the following: (a) the temperature range of validity of the T^3 law is rather limited in most samples studied, (b) the influence of isotopic scattering extends down to the lowest temperatures. Hence, the parameters P, η_E, η, and η_{SC} have been determined by a variational method accounting for *boundary and isotopic scattering*: For this purpose we replace $(1/\tau_B)=(v_B/L_E)$ in the integrals [Eqs. (15)–(17)] by Eq. (22), where now τ_B is a function of P and l. The thermal conductivity is then calculated for different values of P below 10 K and finally the value of P which yields the best fit is chosen for each sample.

Figure 8 displays the results for the samples ^{70}Ge(99.99%) (a) and ^{nat}Ge1 (b) which were subjected to different surface treatments. For ^{nat}Ge1 the treatment was grinding with 20 μm diamond powder slurry, subsequently with 3 μm diamond, then polish etching with SYTON and, finally with CP4. These steps yielded P values of 0.13, 0.15, 0.68, and 0.55. The fitted curves (solid lines in Fig. 8) describe the experimental data well from 2 K to 8 K for the diamond ground surfaces but equally well for CP4 and SYTON treated surfaces in a smaller temperature range (below 4 K). This analysis was performed for all our samples, and in addition, for three Ge samples reported in Ref. 52. Table IV contains the deduced values of P which range from 0.13 ($1.5L_G$) to 0.68 ($5L_G$) for ^{nat}Ge1, and from 0.13 to 0.75 for all other samples, with the exception of $^{70/76}$Ge and ^{70}Ge(95.6%) (Table IV). P has been taken to be independent of phonon frequency and scattering angle in this simplified evaluation.

Ziman[60] and Soffer[62] considered the problem of phonon diffraction by surface irregularities and showed that the specularity depends on the frequency and the angle of phonon incidence. Soffer defined a frequency-dependent probability[62]

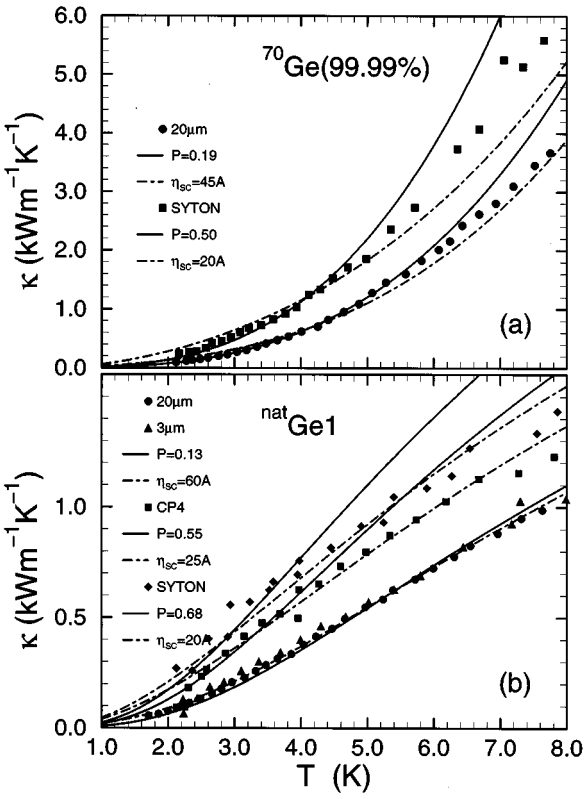

FIG. 8. Model calculations of the effects of specularity on the thermal conductivity below 8 K for Ge samples with different surface treatments (see also Fig. 6 and Fig. 7). The symbols represent the experimental data of ^{70}Ge(99.99%) in (a) and of ^{nat}Ge1 in (b). The solid lines result from the calculations according to Eq. (23) and the dot-dashed lines from the theory of Ziman (Ref. 60) and Soffer (Ref. 62), including frequency and angle dependence, as well as the size correction of phonon boundary scattering.

$$P(k)=\exp[-(2k\eta\cos\Phi)^2],$$

where $\eta\cos\Phi=\eta_E$; k denotes the phonon wave vector, η is the rms height deviation in the surface, and Φ the angle of incidence. Since the temperature gradient is along the sample length $\Phi=(\pi/2)-\Theta$, we obtain the ω dependence of the specularity.

$$P(\omega)=\exp\left[-\left(\frac{2\eta\omega\sin\Theta}{v_i}\right)^2\right], \tag{24}$$

where $i=T,L$, and ω is the phonon frequency and Θ represents the angle between the temperature gradient and the phonon wave vector. The parameter P in Eq. (22) was replaced by $P(\omega)$ and with the integrals [Eqs. (15)–(17)], we computed the thermal conductivity for various values of η_E. For all samples, including those of Ref. 52, this procedure describes $\kappa(T)$ much better than assuming that P is independent of ω. The fitted η_E values are given in Table IV and range from 23 Å (20 μm diamond) to 10 Å (polished with SYTON) for ^{nat}Ge1 and from 35 Å to 8 Å for all samples. This indicates a three times smoother surface for the SYTON treated sample. We remark that η_E is not identical to the geometrical surface roughness but it represents an average value of $\eta\cos\Phi$, which is smaller than the real geometrical roughness.

Frankl and Campisi[52] applied the expression for the specularity factor given by Soffer[62] and determined η_E for ^{nat}Ge samples and Si with differently prepared surfaces but the agreement between their theoretical and experimental data was not very good. Singh and Foshi[59] suggested, that the main reason for the rather poor agreement results from the averaging of the angular dependence of the specularity factor P. In order to solve this problem, they used the exact expression as given by Soffer and the thermal conductivity can be written as:[59]

$$\kappa=\sum_{i=1}^{3}\frac{k_B m^3}{4\pi^2 v_i}T^3\int_0^{\theta_i/T}\frac{x^4e^x}{(e^x-1)^2}dx \times\int_0^{\pi}\tau_C^i(x,\Theta)\cos^2\Theta\sin\Theta\,d\Theta, \tag{25}$$

where the polarization is longitudinal ($i=1$) and transversal ($i=2,3$), $\tau_C^i(x,\Theta)$ is the combined relaxation time for different phonon modes. Singh and Foshi[59] used this expression to determine the values of η and to explain the thermal conductivity of some polished samples of germanium[52] and silicon.[54] However, they did *not* include isotopic scattering and the size correction in their calculations. They found a quite good agreement between their calculations and their experimental data for Ge samples with different treated surfaces below 3 K; for higher temperatures isotopic scattering cannot be neglected. We now performed, for all our samples and those of Ref. 52, calculations of $\kappa(T)$ [using Eq. (25)] by varying η. This procedure includes (a) the integration over the frequency ω *and* the scattering angle Θ of the incident phonons (b) the size correction [Eq. (21)], and finally (c) the consideration of boundary *and* isotopic scattering processes. Figure 8(b) gives the result for ^{nat}Ge1: The calculated $\kappa(T)$ curves (dot-dashed lines) fit well the experimental data below 6 K. The fitted values of η_{SC} (including the size correction) are listed in Table IV. They indicate a rms surface roughness varying from 90 Å to 20 Å. For comparison the η values obtained without size correction (as done in Ref. 59) are also listed in Table IV; they range between 200 Å and 60 Å. Similar analyses for ^{70}Ge(99.99%) and for three samples of ^{nat}Ge with different surface treatments (data taken from Ref. 52 and denoted as ^{nat}GeI, II, and III in Table IV), yield comparable results.

(c) Anisotropy effects observed in the thermal conductivity originate from the elastic anisotropy and the resulting phonon focusing.[54,57,58] Experimental evidence of these effects has been reported for Si.[57] It amounts to a decrease in L_E of 28% for [100] samples and 22% for [110] samples of dimensions similar to those of our samples. Based on the nearly perfect scaling of the dispersions curves,[80] we expect this effect to be similar in Ge.[57]

V. DISCUSSION

This work probably constitutes the most comprehensive study of the effect of isotopic composition on thermal conductivity ever made. We have found that it is possible to represent accurately the $\kappa(T)$ measured for a given sample using different theories and/or various frequency and temperature dependences of the scattering probabilities. In order

to describe $\kappa(T)$ for extremely pure crystals, both terms κ_1 and κ_2 must be taken into account because of the nonresistive nature of normal processes. This requirement restricts the choice of scattering mechanisms, not only for physical but presumably also for mathematical reasons, i.e., so as to avoid the divergence of some of the integrals involved. Physical considerations led us to look for a unique set of coefficients to represent the seven samples studied and other $\kappa(T)$ curves found in the literature.[21] For this purpose neither the model of Callaway[16] nor Holland's modification[19] were successful. We are thus led to a separate treatment of transverse and longitudinal modes (this was also found to be necessary for diamond[22,23,40]) and to take longitudinal Umklapp processes into consideration.

The simultaneous presence of N- and U-type scattering is thus crucial for successful curve fitting. Both, N and U processes are needed so that the thermal conductivity integrals give meaningful results when the full form of the Callaway theory is used. The longitudinal Umklapp processes are indispensable to obtain the strong decrease of $\kappa(T)$ with T observed at higher temperatures. We find that the exponent n of the temperature dependence for the Umklapp scattering rate ($B_{iU}\omega^2 T^n \exp^{-C_i/T}$, $i=T,L$) strongly influences $\kappa(T)$ above the maximum. From theoretical models, values between $n=-1$ and $n=6$ have been reported, we only find $n=1$ acceptable for fitting our data, in agreement with the results in Refs. 23,71,72,74. This conclusion supports suggestions[14,36,43,75,38] that while the heat flow above the maximum of $\kappa(T)$ is primarily due to transverse phonons, longitudinal Umklapp processes also play a role. Using the parameters of Table III we find that τ_N^{-1} is much larger ($\sim$ three orders of magnitude) than τ_U^{-1}. Similar conclusions have been reached for diamond.[23]

B_{LU} and B_{TU} were fitted independently since there is no reason why they should be equal, although they may be expected to be of the same order of magnitude. C_T and C_L (appearing in the exponential factor of the Umklapp processes) were taken to be different, scaling like the Debye temperatures for the corresponding T and L branches, $\theta_T=118$ K and $\theta_L=333$ K. Usually the exponent C_i is denoted as $C_i=\theta/x$ with $2<x<6$, depending on the power of the temperature, taken from the literature.[53] Our fits yield an x value of about 3, the value of x most frequently found in the literature. Isotope effects are clearly detected at low and at high temperatures (300 K). The measured variation of κ_m with the mass variance g (Fig. 3) clearly confirms, over a large range of isotopic compositions, that the isotopic scattering is well represented by the point defect theory of Klemens.[35] At low temperatures the measured curves show a T^2 to T^3 dependence for $\kappa(T)$; the deviation from T^3 expected for boundary scattering originates from isotopic scattering alone. A higher value of the mass variance g shifts the overall $\kappa(T)$ curve towards lower thermal conductivities, while κ_m occurs at slightly lower temperatures and, consequently, the range of T^3 dependence begins at lower temperatures (Figs. 1 and 3).

Our modified Callaway/Holland formalism describes the effect of isotopic disorder at any temperature below 200 K. (This becomes obvious from Fig. 3 which shows the κ_m values vs the variance g and the influence of the effective phonon mean free path L_E and dislocations.) Within the experimental errors, the influence of dislocations on κ_m is negligible when $g>10^{-4}$, the general case for the samples studied. Sample $^{70/76}$Ge has a lower κ_m (a) for geometrical reasons (with $L_E=0.7$ mm) since cross section and length are much smaller than those of the other samples studied (see Table I) and (b) due to its [110] orientation.

The $\kappa(T)$ curves fitted as described above give around the maximum values somewhat higher than the experimental ones. The largest deviation is observed for ^{70}Ge(99.99%) where the calculated κ_m exceeds the experimental data by a factor of two [Fig. 4(a) and Fig. 5(a)]. We interpret this as the effect of additional scattering mechanisms, in particular, the presence of dislocations.

The fitted curves obtained, using the model of Holland with $\kappa(T)=\kappa_1$ ($\kappa_2=0$) also surpass the measured data with the exception of the isotopically pure ^{70}Ge(99.99%) sample for which the opposite was observed. In order to improve the fits we had to assume a variation of the prefactor of the normal processes with g: This prefactor (B_T) for ^{70}Ge(99.99%) turned out to be half the value of that found for other isotopic compositions. This dependence of B_T disappeared when using ''Model 1'' at the expense of deviations. Dislocation scattering is the most reasonable among the possible mechanisms which can be invoked to eliminate these deviations (see Fig. 3 and Fig. 5). The calculated thermal conductivities are barely changed by weak dislocation scattering, with the exception of ^{70}Ge(99.99%). The difference between the curves calculated with and without dislocations disappears quickly with increasing g. It is not detectable for $^{70/76}$Ge, as displayed in Fig. 5(b) and also not for all other samples.

Similar procedure has been used to calculate the κ_m as a function of g for dislocation-free crystals. The results are shown as a continuous line in Fig. 3 for different values of L_E. We deduce $\kappa_m \approx 12$ kW/mK for $g=10^{-6}$, and $\kappa_m \approx 20$ kW/mK for $g=10^{-7}$ under the assumption, that there are no dislocations. Assuming $L_E=3.6$ mm and a dislocation-free sample of ^{70}Ge(99.99%), then the thermal conductivity is about 20 kW/mK near 20 K, instead of the 10.5 kW/mK found experimentally.

The results given in Figs. 6 to 8 and listed in Table IV underscore the importance of surface preparation on the magnitude of $\kappa(T)$ near and below κ_m for samples with sufficient isotopic purity. The theory of the Ziman[60] and Soffer[62] enables us to describe the influence of the various degrees of surface polishing on the temperature dependence of $\kappa(T)$ for all samples with a given geometry and mass variance. A single parameter, the specularity factor P, is sufficient to account for effects resulting from the surface roughness.

The enhancement of κ due to specular reflection is considerably larger at the lower temperatures than at higher ones. An interesting feature is the observation that the higher the boundary-limited thermal conductivity, the lower the temperature below which the T^3 law is valid (Fig. 1).

Inspection of the samples with [100] orientation in Table IV gives $0.13 \leqslant P \leqslant 0.28$ as typical values for samples which have been sand blasted or ground with 3 μm to 20 μm diamond powder slurry. Samples treated with 1 μm diamond or CP4 ($^{\mathrm{nat}}$GeII,$^{\mathrm{nat}}$Ge1) yield $P \simeq 0.5$, and the samples pol-

ished with SYTON or LUSTROX (Ref. 81) show the best surface performance with $P \geqslant 0.7$ (^{nat}Ge1, ^{nat}GeII). Sample ^{70}Ge(99.99%), also polished with SYTON, does not fit into this scheme since $P = 0.5$. This can be explained by the influence of dislocation scattering which is very pronounced in this sample. There is overall agreement between our data and the earlier reports in Refs. 6,7,52,55. The improvement of $\kappa(T < 10$ K) between sand-blasted and best-polished samples of Ge along the [100] direction amounts to a factor of three.

With regards to the effect of sample orientation on the thermal conductivity the data of L_E in Table IV seems to confirm the results reported by Frankl and Campisi[52] that germanium, with an orientation in either the [110] (or the [111]) direction, possesses near 2 K a $\kappa(T)$ which is only 75% or (50%) of that for a sample oriented along [100] [see also κ(3 K) in Table I]. Our samples ^{70}Ge(95.6%) and $^{70/76}$Ge are oriented along [110] and fit into this scheme. Recently, it was observed that for Ge with natural isotopic composition the thermal conductivity in [100] direction is 50% higher than in the [111] direction below T_m.[82] For all samples studied (Table IV) $L_C \leqslant L_E$ with the exception of ^{70}Ge(95.6%). For this sample we could not find suitable values for the surface characterization, to fit the low temperature data, because of the influence of electronic carrier scattering ($p \approx 10^{16}$ cm^{-3}). Unfortunately, the number of samples presently available to us is insufficient to make any more precise statements on the orientational anisotropy of $\kappa(T)$. For this purpose isotopically pure samples of various orientations would be required.

VI. CONCLUSIONS

The present analysis of the thermal conductivity of Ge samples with several isotopic compositions, using a modified Callaway/Holland formalism, works well below 200 K. A single set of parameters describes the interplay of the different scattering mechanisms even when individual contributions vary over a wide range, e.g., isotopical disorder, geometry, etc. The modified Callaway/Holland model enables us to predict $\kappa(T)$ for a Ge sample with defined geometry and isotopic composition, and leads to the following conclusions:

(a) The full form of the Callaway integrals ($\kappa_1 + \kappa_2$) must be computed in the case of isotopically pure samples (normal scattering processes are not entirely resistive) in order to obtain meaningful results for $\kappa(T)$. The separation into transverse and longitudinal modes is necessary.

(b) Normal processes and longitudinal Umklapp processes cannot be neglected.

(c) The detailed structure of the phonon density of states does not play a significant role in the representation of $\kappa(T)$. The use of a more realistic phonon dispersion, instead of the Debye spectrum (as done by Holland), does not improve the agreement between measured and calculated data.

(d) The temperature and frequency dependences for the individual scattering mechanisms proposed by Klemens[15] and Herring[14] are supported by this study.

(e) Isotopic scattering cannot be neglected in the analysis of the low temperature thermal conductivity of germanium.

(f) The effects of sample geometry, surface treatment (roughness), dislocation density, and orientation are strongly enhanced with increasing isotopic purity since these parameters govern the effective phonon mean free path, and therefore $\kappa(T)$, near and below T_m. Specular reflection can be treated by the theory of Ziman[60] and Soffer.[62]

(g) The improvement of $\kappa(T)$ by optimized surface treatment, e.g., polish etching with SYTON, does barely exceed a factor of two; the geometrical parameters are dominant.

(h) The Callaway method is not adequate for higher energy phonons: It overestimates scattering rates and thus underestimates $\kappa(T)$. Any extra scattering mechanism, e.g., multiple phonon scattering, would tend to reduce $\kappa(T)$ even further. A description of $\kappa(T)$ over a wider range of T would require a much more structured dependence of the scattering parameters over that T range and the whole Brillouin zone. The complexity of the scattering processes involved and their interplay (by the integrals) makes it unlikely at present to find any better procedure of comparable simplicity.

In summary, we have presented measurements of the thermal conductivity $\kappa(T)$ of high purity germanium single crystals with several isotopic concentrations covering the range from maximum mass variance ($^{70/76}$Ge) to high isotopic purity (^{70}Ge(99.99%)). The latter sample has been shown to exhibits an increase in κ_m (found at 16.5 K) by a factor of ≈ 8 with respect to natural germanium, while for the $^{70/76}$Ge sample κ_m is 1.8 times lower. The results have been fitted to a modified Callaway/Holland theory with three adjustable parameters for each phonon branch to describe anharmonic phonon scattering. A detailed investigation of the low temperature region has allowed us to obtain values of the effective sample cross section which is enhanced compared to the geometrical one by effects of focusing plus finite sample length. This cross section increases when coarse ground sample surfaces are polish etched with SYTON. The results have been compared with other available data for natural Ge[52] and with early results for an isotopically enriched ^{74}Ge sample.[21]

ACKNOWLEDGMENTS

The authors thank E. Schmitt for skillful help with the measurements, K. Rössmann for helpful advice with computer programs. They also gratefully acknowledge financial support from the European Union through the INTAS agency and from Max-Planck Research. The isotopically controlled Ge single crystals were grown at the Lawrence Berkeley National Laboratory operated by the University of California under DOE Contract No. DE-AC03-765F00098.

*Present address: Keio University, 3-14-1 Hiyoshi, Kohokuku, Yokohama 223, Japan.

[1] M. G. Holland, in *Physics of III-V Compounds*, edited by R. K. Willardson and A. C. Beer, Semiconductor and Semimetals Vol. 2 (Academic Press, New York, 1966), p. 3.

[2] P. Carruthers, Rev. Mod. Phys. **33**, 92 (1961).

[3] J. R. Drabble and H. J. Goldsmith, in *Thermal Conduction in Semiconductors* (Pergamon Press, Oxford, 1961).

[4] G. A. Slack and C. Glassbrenner, Phys. Rev. **120**, 782 (1960).
[5] C. J. Glassbrenner and G. A. Slack, Phys. Rev. **134**, A1 058 (1964).
[6] J. A. Carruthers, T. H. Geballe, H. M. Rosenberg, and J. M. Ziman, Proc. R. Soc. London, Ser. A **238**, 502 (1957).
[7] B. L. Bird and N. Pearlman, Phys. Rev. B **4**, 4406 (1971).
[8] *Semiconductors, Intrinsic Properties of Group IV Elements and III-V, II-VI and I-VII Compounds*, edited by K.-H. Hellwege and O. Madelung, Landolt-Börnstein, New Series, Group III, Vol. 22, Pt. a (Springer, Berlin, 1987), p. 281.
[9] Y. S. Touloukian, R. W. Powell, C. Y. Ho, and P. G. Klemens, in *Thermophysical Properties of Matter Vol. 1, Thermal Conductivity* (IFI/Plenum, New York, 1970), p. 108.
[10] L. J. Challis, A. M. de Goer, and S. C. Haseler, Phys. Rev. Lett. **39**, 558 (1977).
[11] J. F. Goff and N. Pearlman, Phys. Rev. **140A**, 2151 (1965).
[12] R. E. Peierls, Ann. Phys. (Leipzig) **3**, 1055 (1929).
[13] P. G. Klemens, in *Solid State Physics: Advances in Research and Applications*, edited by F. Seitz and D. Thurnbull (Academic Press, New York, 1958), Vol. 7, pp. 1–99.
[14] C. Herring, Phys. Rev. **95**, 954 (1954).
[15] P. G. Klemens, Proc. R. Soc. London, Ser. A **208**, 108 (1951).
[16] J. Callaway, Phys. Rev. **113**, 1046 (1959).
[17] J. Callaway and H. C. von Baeyer, Phys. Rev. **120**, 1149 (1960).
[18] J. Callaway, Phys. Rev. **122**, 787 (1961).
[19] M. G. Holland, Phys. Rev. **132**, 2461 (1963).
[20] I. Pomeranchuk, J. Phys. (Moscow) **5**, 237 (1942).
[21] T. H. Geballe and G. W. Hull, Phys. Rev. **110**, 773 (1958).
[22] J. R. Olson, R. O. Pohl, J. W. Vandersande, A. Zoltan, T. R. Anthony, and W. F. Banholzer, Phys. Rev. B **47**, 14 850 (1993).
[23] L. Wei, P. K. Kuo, R. L. Thomas, T. R. Anthony, and W. F. Banholzer, Phys. Rev. Lett. **70**, 3764 (1993).
[24] J. E. Berman, J. B. Hastings, D. P. Siddons, M. Koike, V. Strojanoff, and S. Sharma, Synch. Rad. News **6**, 21 (1993).
[25] J. Bigeleisen, M. W. Lee, and F. Mandel, Annu. Rev. Phys. Chem. **24**, 407 (1973).
[26] K. Itoh, W. L. Hansen, E. E. Haller, J. W. Farmer, V. I. Ozhogin, A. Rudnev, and A. Tikhomirov, J. Mater. Res. **8**, 1341 (1993), and references therein.
[27] M. Cardona, in *Advances in Solid State Physics*, edited by R. Helbig (Vieweg, Braunschweig, 1995), Vol. 34, p. 35.
[28] E. E. Haller, J. Appl. Phys. **77**, 2857 (1995).
[29] A. A. Berezin, J. Phys. Chem. Solids **50**, 5 (1988).
[30] P. Etchegoin, H. D. Fuchs, J. Weber, M. Cardona, L. Pintschovius, N. Pyka, K. Itoh, and E. E. Haller, Phys. Rev. B **48**, 12 661 (1993).
[31] H. D. Fuchs, C. H. Grein, M. Cardona, W. L. Hansen, K. Itoh, and E. E. Haller, Solid State Commun. **82**, 225 (1992).
[32] P. Etchegoin, J. Weber, M. Cardona, W. L. Hansen, K. Itoh, and E. E. Haller, Solid State Commun. **83**, 843 (1992).
[33] H. D. Fuchs, P. Etcheogin, M. Cardona, K. Itoh, and E. E. Haller, Phys. Rev. Lett. **70**, 1715 (1993).
[34] H. D. Fuchs, C. H. Grein, R. I. Devlen, J. Kuhl, and M. Cardona, Phys. Rev. B **44**, 8633 (1991).
[35] P. G. Klemens, Proc. Phys. Soc. London, Sect. A **68**, 1113 (1955).
[36] R. Berman and J. C. F. Brock, Proc. R. Soc. London, Ser. A **289**, 46 (1965).
[37] S. R. Bakhchieva, N. E. Kekelidze, and M. G. Kekua, Phys. Status Solidi A **83**, 139 (1984).
[38] B. Abeles, Phys. Rev. **125**, 44 (1962).
[39] J. W. Vandersande, Phys. Rev. B **15**, 2355 (1977).
[40] J. E. Graebner, M. E. Reiss, L. Seibles, T. M. Hartnett, R. P. Miller, and C. J. Robinson, Phys. Rev. B **50**, 3702 (1994).
[41] R. Berman, C. L. Bounds, and S. J. Rogers, Proc. R. Soc. London, Ser. A **289**, 66 (1965).
[42] R. Berman, C. L. Bounds, C. R. Day, and H. H. Sample, Phys. Lett. **26A**, 185 (1968).
[43] P. D. Thacher, Phys. Rev. **156**, 975 (1967).
[44] R. Berman, E. L. Foster, and J. M. Ziman, Proc. R. Soc. London, Ser. A **237**, 344 (1956).
[45] R. M. Kimber and S. J. Rogers, J. Phys. C **6**, 2279 (1973).
[46] H. D. Jones, Phys. Rev. A **1**, 71 (1970).
[47] G. S. Karumidze and L. A. Shengelia, Diam. Relat. Mater. **3**, 14 (1993).
[48] V. G. Manzhelii, B. Ya. Gorodilov, and A. I. Krivchikov, Low Temp. Phys. **22**, 131 (1996), and references therein.
[49] A. P. Zhernov, Phys. Status Solidi B **193**, 311 (1996), and references therein.
[50] B. B. G. Casimir, Physica (Utrecht) **5**, 495 (1938).
[51] R. Berman, F. E. Simon, and J. M. Ziman, Proc. R. Soc. London, Ser. A **220**, 171 (1953).
[52] D. R. Frankl and G. J. Campisi, in *Proceedings of the International Conference on Phonon Scattering in Solids, Paris, 1972*, edited by H. J. Albany (La Documentation Française, Paris, 1972), pp. 88–93.
[53] R. Berman, in *Thermal Conductivity in Solids* (Oxford University Press, Oxford, 1976).
[54] W. S. Hurst and D. R. Frankl, Phys. Rev. B **186**, 801 (1969).
[55] G. J. Campisi and D. R. Frankl, Phys. Rev. B **10**, 2644 (1974).
[56] R. Berman, E. L. Foster, and J. M. Ziman, Proc. R. Soc. London, Ser. A **231**, 130 (1955).
[57] A. K. McCurdy, H. J. Maris, and C. Elbaum, Phys. Rev. B **2**, 4077 (1970).
[58] B. Taylor, H. J. Maris, and C. Elbaum, Phys. Rev. Lett. **23**, 416 (1969).
[59] D. P. Singh and Y. P. Foshi, Phys. Rev. B **19**, 3133 (1979).
[60] J. M. Ziman, Can. J. Phys. **34**, 1256 (1956).
[61] J. M. Ziman, in *Electrons and Phonons* (Clarendon Press, Oxford, 1979).
[62] S. B. Soffer, J. Appl. Phys. **38**, 1710 (1967).
[63] Y.-J. Han and P. G. Klemens, Phys. Rev. B **48**, 6033 (1993).
[64] R. L. Sproull, M. Moss, and H. Weinstock, J. Appl. Phys. **30**, 334 (1959).
[65] G. K. White, in *Thermal Conductivity of Solids*, edited by R. P. Tye (Academic Press, London, 1969).
[66] G. K. White and S. B. Woods, Phys. Rev. **103**, 569 (1956).
[67] R. Berman, E. L. Foster, B. Schneidmesser, and S. M. A. Tirmizi, J. Appl. Phys. **31**, 2156 (1960).
[68] H. E. Jackson and C. T. Walker, Phys. Rev. B **3**, 1428 (1971).
[69] S. Tamura, Phys. Rev. B **27**, 858 (1983).
[70] R. O. Pohl, Z. Phys. **176**, 358 (1963).
[71] R. Berman, F. E. Simon, and J. Wilks, Nature (London) **168**, 277 (1951).
[72] F. J. Webb, K. R. Wilkinson, and J. Wilks, Proc. R. Soc. London, Ser. A **214**, 546 (1952).
[73] G. Nelin and G. Nilsson, Phys. Rev. B **5**, 3151 (1972).
[74] D. G. Onn, A. Witek, Y. Z. Qui, T. R. Anthony, and W. F. Banholzer, Phys. Rev. Lett. **68**, 2806 (1992).
[75] J. E. Parrot, Proc. Phys. Soc. London **81**, 726 (1963).
[76] B. Abeles, Phys. Rev. **131**, 1906 (1963).

[77] SYTON is a trademark of Monsanto Company.
[78] H. C. Gatos and M. C. Lavine, in *Progress in Semiconductors*, edited by A. F. Gibson and R. E. Burgess (Heywood Book, London, 1965), Vol. 9; F. L. Vogel, W. Pfann, W. G. Corey, and E. E. Thomas, Phys. Rev. **90**, 489 (1953).
[79] T. Klitsner, J. E. VanCleve, H. E. Fischer, and R. O. Pohl, Phys. Rev. B **38**, 7576 (1988).
[80] G. Nelin and G. Nilsson, Phys. Rev. B **6**, 3777 (1972).
[81] Lustrox sold by Tizon Chemical Company Flemington, New Jersey, USA.
[82] V. Ozhogin (private communication).
[83] M. G. Holland, Bull. Am. Phys. Soc. **8**, 15 (1963).